

LA-UR-19-29163

Approved for public release; distribution is unlimited.

Title: Performance of BaFCl:Eu²⁺ scintillating composites for X-ray imaging screens

Author(s): Richards, Cameron Gregory

Intended for: Report

Issued: 2019-09-12

Disclaimer:

Los Alamos National Laboratory, an affirmative action/equal opportunity employer, is operated by Triad National Security, LLC for the National Nuclear Security Administration of U.S. Department of Energy under contract 89233218CNA000001. By approving this article, the publisher recognizes that the U.S. Government retains nonexclusive, royalty-free license to publish or reproduce the published form of this contribution, or to allow others to do so, for U.S. Government purposes. Los Alamos National Laboratory requests that the publisher identify this article as work performed under the auspices of the U.S. Department of Energy. Los Alamos National Laboratory strongly supports academic freedom and a researcher's right to publish; as an institution, however, the Laboratory does not endorse the viewpoint of a publication or guarantee its technical correctness.

Performance of BaFCl:Eu²⁺ scintillating composites for X-ray imaging screens

CAMERON G. RICHARDS,^{1,2,*}

¹*Graduate Research Intern, MST-7 Engineered Materials, Los Alamos National Laboratory, Bikini Atoll Rd., SM 30, Los Alamos, NM 87545, USA*

²*Optical Materials and Devices, Masters Industrial Internship Program, 1252 University of Oregon Eugene, OR 97403, USA*

**crichar7@uoregon.edu*

Abstract:

A cost-effective solution for improving X-ray imaging detectors is presented through the use of a translucent scintillating composite and pixelated screen structure. A large quantity of BaFCl:Eu²⁺ polycrystalline scintillator powder was synthesized via flux growth and its optical properties characterized through photoluminescence (PL) and absolute quantum yield (QY). UV-curable composites containing the BaFCl:Eu²⁺ material were fabricated with differing amounts of NOA1665 and NOA170 optical adhesives. It was determined that, when the two resins were combined, the translucency of the resulting composite could be enhanced. The BaFCl:Eu²⁺ composite was also cast into a pixelated glass screen containing an array of 160 μm x 160 μm holes by two separate methods: composite paste application and powder-resin application. Based on visual inspection, using a composite paste to fill the apertures proved to be more effective in creating a uniform packing.

1. Introduction

1.1 Engineering Advancements to Radiographic Detection

X-ray imaging techniques applicable to the medical industry, such as computed tomography (CT), have undergone significant reformation and development over the past few decades. With global concerns over the detrimental effects of radiation exposure and cancer related illnesses, new materials and designs are being developed to help reduce the risks associated with radiometric practices. Parallel to this effort, modern research is driven by the need for faster, more efficient, and more cost effective solutions pertaining to detector elements within the X-ray imaging process. Inherently, these demands are highly complex and require a multi-faceted approach in order to meet them.

Here, we discuss a two-fold design improvement to modern X-ray detectors; the first of which is a materials development, and the second an engineering refinement. In 1983, *Cusano et al.* [3] proposed an idea for a composite scintillating material containing an optical binding agent and scintillator of equal refractive indices. This index-matching condition creates a more translucent medium for visible photon propagation by reducing scattering events due to interfacial reflections at surface boundaries. The increase in the optical light transport can lead to a substantially greater detector response, improve image quality, and reduce the necessary measurement time. Generally, activator-type inorganic scintillators, such as those commonly used for X-ray detection, typically have high refractive indices (1.8-2+) [9] whereas the indices of most commercial binders lie below 1.7. For this reason, among others discussed later, we explore the use of BaFCl:Eu²⁺ since its refractive index lies between 1.65 and 1.71 over the visible spectrum. Fig. 1 shows the dispersion curve for BaFCl:Eu²⁺ with the indices of two commercially available optical adhesives for reference.

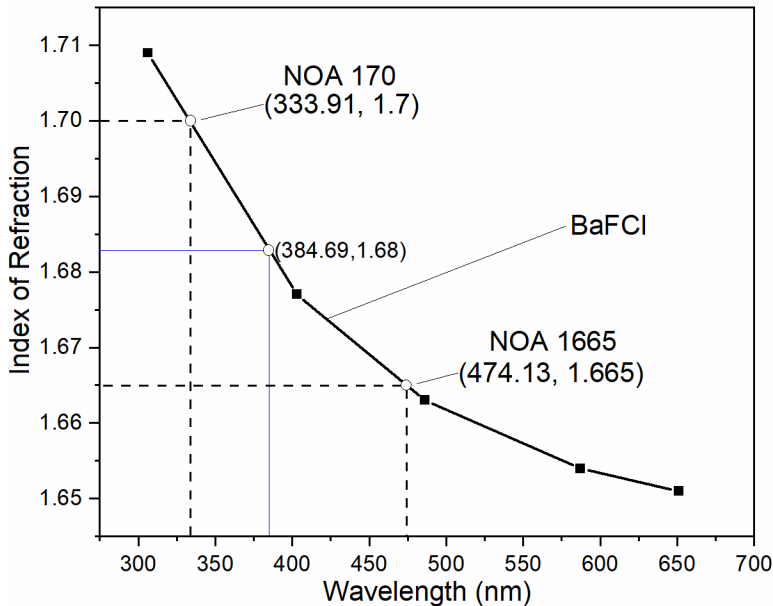


Fig. 1. Dispersion curve of BaFCl:Eu^{2+} over the visible spectrum. Norland Optical Adhesives 1665 and 170 are included for reference. Work in this paper explores mixing the two resins to match the index of BaFCl:Eu^{2+} at 385 nm (the primary emission wavelength of the Eu^{2+} ion).

In addition to the potential improvements resulting from using a translucent composite, the use of a pixelated screen in conjunction with the composite can further enhance the detection capability. Pixelated structures are advantageous due to the fact that they can enhance spatial resolution by constraining the visible photons within pillar-like structures; this geometry can be used to directly align an array of photo-detectors. A reflective surface bordering the pillar can further improve the number of visible photons reaching the detector by redirecting the light towards the detector pixel. Hence, by channeling the visible light in the effective waveguide, cross-talk between pixels can be reduced and signal-to-noise can be improved.

A variety of designs utilizing this concept have been explored, ranging from modular systems to rigid structures [19]. Each design exhibits unique features which make it innovative; however, careful considerations on the cost must also be made. Many of the “modern” detector designs incorporate very expensive materials (i.e. tungsten, single-crystal scintillators) and could easily take on the order of months to fully construct. Therefore, a relatively quick and cost-effective solution is to use a lithographically formed pixelated screen and fill the apertures with a composite scintillator. The benefits of this route are that the scintillator can be formed as a polycrystalline material, the composite can be easily applied into the screen, and the whole process can be done on the order of weeks.

1.2 Optical Properties of BaFCl:Eu^{2+}

The europium-doped barium fluoro-halides (BaFBr:Eu^{2+} , BaFCl:Eu^{2+}) have been known to actively produce scintillation photons for over 30 years [20]. Since the time of their discovery, an extensive amount of research has rendered a desirable level of maturity for their properties. It is well known [1, 2, 5, 7, 13, 16-18, 20] that under UV- and X-ray irradiation, BaFCl:Eu^{2+} typically exhibits luminescence emissions near 365 nm, 385 nm, and occasionally 430 nm due to electronic transitions of the Eu^{2+} activator ion. These emission wavelengths are subject to broadening and shifts resulting from solid-state system effects. The lifetimes of the 385 nm and 430 nm emissions have been reported to be in the μs and sub- μs regime, respectively [17].

These values were confirmed in the last paper using Time-Correlated Single Photon Counting (TCSPC), yielding primary lifetime decay constants of 2.947 μ s and 0.4719 μ s for the 385 nm and 430 nm emissions. The speed, emission wavelengths, and stability in atmosphere make BaFCl:Eu²⁺ a suitable choice for the radiographic applications.

Previous studies on the effects of synthesis parameters on the optical properties of BaFCl:Eu²⁺ indicated a correlation between the luminescence and structural properties of the crystal; extended dwelling time provided sufficient conditions for the nucleation of an alternate phase (Ba₁₂F₁₉Cl₅). The presence of this Ba₁₂F₁₉Cl₅ phase can be related to the reported 430 nm emission. With reduced dwell time, the 430 nm emission was no longer present and the intensity of the 385 nm emission increased three-fold. The discovery of the secondary phase was found through XRD analysis and supported by recent literature discussing the secondary phase [11]. Other research [4, 8] has suggested oxygen impurities can migrate into the crystal, leading to similar shifts in the transition energies. Future work may be performed to investigate the properties of the secondary phase and to elucidate the true origin of the 430 nm transition.

1.3 BaFCl:Eu²⁺ Scintillating Composites

A composite material utilizing the synthesized BaFCl:Eu²⁺, Norland Optical Adhesive 1665 (NOA 1665), and IPA was previously fabricated and optimized for balanced translucency and density. In the previous paper, it was determined that a 50% by weight contribution of IPA and 50% volume fraction of NOA 1665 to the total volume yields the desired traits. These values were based on UV-VIS absorption spectroscopy and radio-luminescence spectroscopy.

For the intended application, it is necessary to maintain a particle size less than 40 μ m to ensure adequate filling and packing of the screen apertures. Due to the large distribution of sizes following the synthesis, post processing of the powder is necessary. Currently, the powder is crushed by hand using a mortar and pestle. Though effective for reducing size, it was also shown in the previous work that this technique may quench the luminescence intensity by up to 30% after multiple iterations. Therefore post synthesis crushing is kept to a minimum to maintain optical quality.

2. Experimental

2.1 BaFCl:Eu²⁺ Composite Fabrication

A large scale flux growth synthesis of BaFCl:Eu²⁺ was performed with BaF₂(s), BaCl₂(s), and EuF₂(s) reagents. The constituents were mixed in a large glassy carbon crucible and allowed to dwell at 1100°C for 2 hours. Polycrystalline BaFCl:Eu²⁺ is formed during cooling. Once fully cooled, the yield was crushed and washed with DI water to filter out excess BaCl₂. Subsequent annealing of the scintillator yield at 120°C dehydrated the material. PL emission spectra were obtained for multiple samples of the synthesis yield on a Photon Technology Inc. fluorescence spectrometer. The yield was then crushed and sieved to isolate particle size distributions. Four particle size subsets were created using a multi-layered sieve with mesh sizes 75 μ m, 53 μ m, and 38 μ m. Only powder from the smallest subset was used for further experimentation.

The quantum yield, or ratio of photons emitted to photons absorbed, of the BaFCl:Eu²⁺ powder was measured on a Hamamatsu Quantarus-QY Absolute PL Quantum Yield Spectrometer C11347 system. The excitation wavelength was set to 335 nm for all measurements, corresponding to the wavelength for maximum excitation. To account for variation within the system, the sample was rotated by 45° after every 10 measurements, subtending a full 360°. A total of 90 measurements were taken.

Following scintillator characterization, composite pastes consisting of the BaFCl:Eu²⁺ powder, NOA 1665, NOA 170, and IPA were fabricated. For each mixture, a 50% volume fraction (V_f) of resin was maintained. Composites with varying mass ratios of NOA 1665/NOA 170 resins were made. The ratios included in the study were 100/0, 75/25, and 50/50. The mixing procedure, seen in Table 1, was performed in a Thinky Planetary Vacuum Mixer. IPA was included to dissipate heat during mixing and to improve uniformity of the resulting composite.

Two methods for applying the scintillator into a pixelated glass screen with a lithographically formed array of 160 μm x 160 μm holes were tested. In the first method, a composite paste was applied via sheer force onto the glass screen. For the second method, BaFCl:Eu²⁺ powder (<38 μm) was placed directly onto the screen and was agitated to allow the powder to fall into the holes; after this step, NOA 1665 resin was then poured over the region containing the powder to fill the void space. Uniformity of the packing was done through visual inspection.

Table 1. Thinky Mixer cycle for composite paste development.

Step	Speed (rpm)	Vacuum (kPa)	Duration (min.sec)
1	2000	Off	0.30
2	500	Off	2.00
3	2000	Off	0.30
4	500	0.2	2.00
5	2000	0.2	0.30

3. Results and Discussion

3.1 BaFCl:Eu²⁺ Synthesis and Characterization

The large-scale flux growth synthesis of BaFCl:Eu²⁺ produced roughly 90 g of the polycrystalline scintillator. After filtering, crushing, and sieving, more than 25 g of powder within the <38 μm subset was isolated (see Fig. 2). PL emission characteristics were very similar to those of previous batches, indicating a successful synthesis. It was predicted that, due to the scale up, the 2 hour dwell time would produce similar results to those of the 30 minute dwell time performed previously with a smaller batch. Seen below in Fig. 3, the PL spectra exhibits the two main peaks at 365 nm and 383 nm, due to the $^6\text{P}_{7/2} \rightarrow ^8\text{S}_{7/2}$ and $4\text{f}^65\text{d}^1 \rightarrow ^8\text{S}_{7/2}$ electronic transitions of Eu²⁺ ions. The peak at 383 nm is substantially broader as a result of the crystal field effect, which is known to cause shifts in electronic transition energies of the luminescent ions. It can also be seen in the plot that within the yield there is less than a 5% variation in the PL intensity, suggesting good uniformity throughout the batch.

Quantum yield (QY) measurements of the BaFCl:Eu²⁺ powder resulted in an average absolute QY of 44.8% with a standard deviation of 0.7%. Based on these results, it can be expected that for every 3 photons absorbed by the BaFCl:Eu²⁺, on average 2 photons will be reemitted. While a direct correlation between QY and light yield cannot be established, this information provides a higher confidence that the scintillator is able to transfer energy efficiently to the luminescent ions. Since the excitation wavelength is near resonance with the luminescence transitions, this is the ideal case. It is likely that the QY value will reduce when exciting with higher energies (i.e. X-rays), due to the inefficiencies of energy transfer within the crystal.

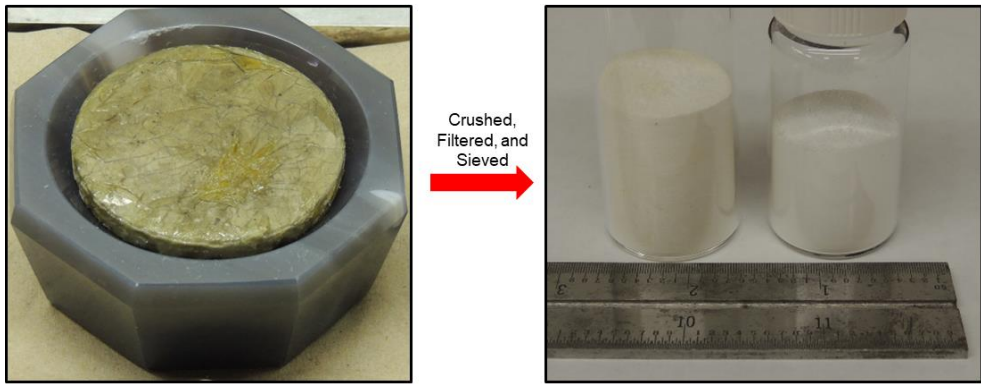


Fig. 2. (left): Photograph of the large-scale BaFCl:Eu^{2+} synthesis yield prior to post-processing. (right): BaFCl:Eu^{2+} polycrystalline powder after post-processing. Over 25 g of the material is under 38 μm in size and is within the container on the right.

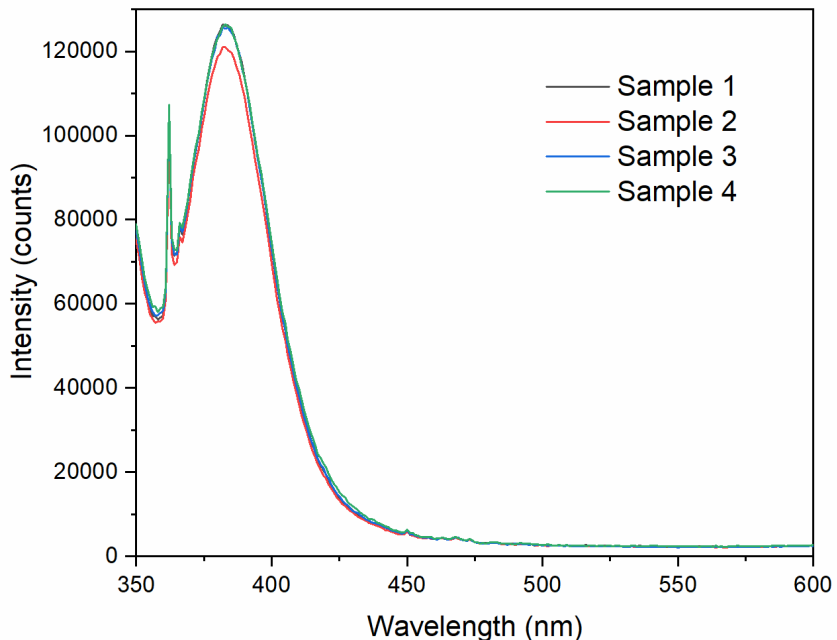


Fig. 3. Photoluminescence spectra of multiple samples from the BaFCl:Eu^{2+} synthesis. The variation in peak intensity is less than 5%.

3.2 Composite Fabrication and Performance

Here, it was determined that the IPA study performed previously was more complicated than originally thought. Large quantities of IPA were initially shown to reduce the composite translucency, and that parameter continues to hold true; however, that result is also time dependent. Due to the evaporation of IPA, the composite was constantly undergoing a viscosity and chromatic change following the initial mixing. As time progressed, the viscosity of the composite increased as more IPA evaporated. Additionally, the coloration changed from a gray, opaque hue to a more green translucent appearance. The rate at which IPA evaporated was calculated to be approximately 0.1 mg/s, as shown in Fig. 4.

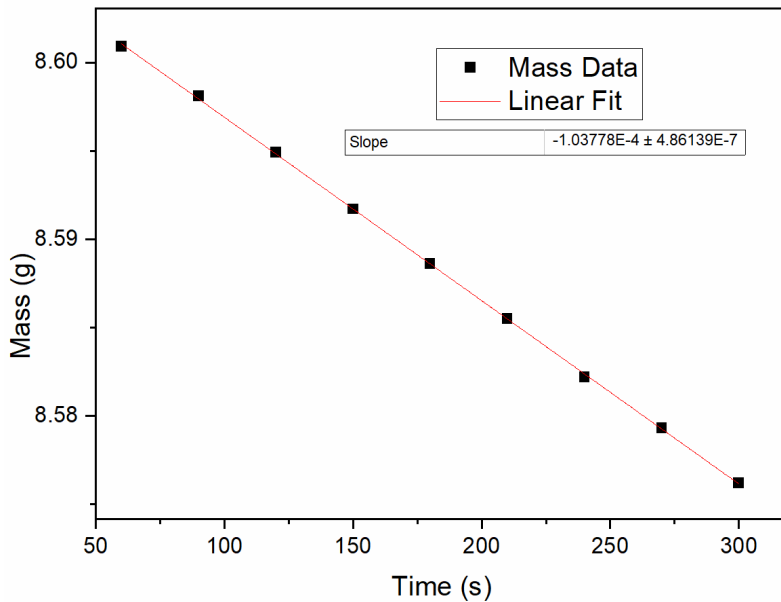


Fig. 4. Linear fit of the recorded mass data from one of the composites formed with excess IPA. The rate at which IPA evaporated was calculated to be approximately 0.104 mg/s.

Composites fabricated during the mixed resin study showed significant improvement in both uniformity and translucency. Shown below in Fig. 5, the composites are arranged from left to right in order of increasing NOA 170 contributions under ambient (top) and UV (bottom) illumination. For each composite, the translucency under UV exposure appears very uniform and can be attributed to the increase in IPA during the mixing process. The white regions located in the 75/25 mix and 50/50 mix are due to slight damage incurred while removing from the application surface. Sufficient evidence for an improved index matching condition within the composite was found through UV-VIS absorption spectroscopy, shown in Fig. 6, where both mixed resin composites had a reduction in the total absorption.

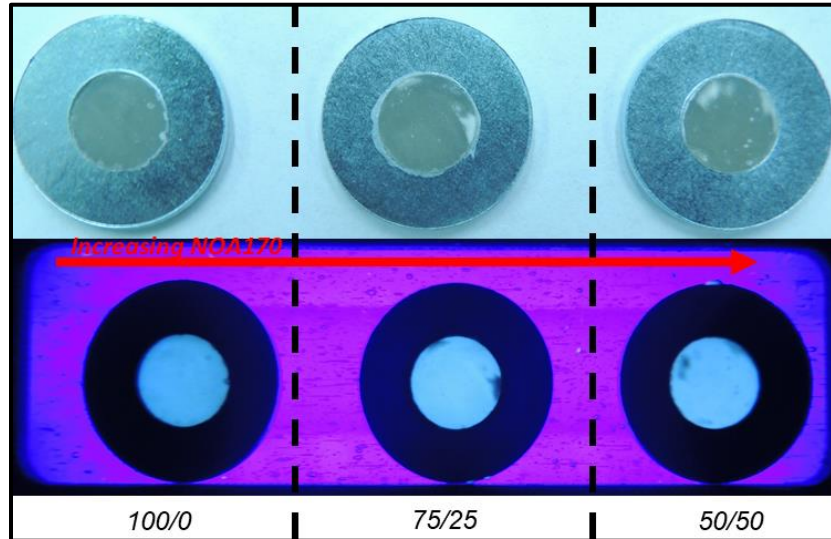


Fig. 5. Photograph of the composites made for the mixed resin study. Composites are arranged from left to right in order of increasing NOA 170 under ambient (top) and UV (bottom) illumination. The ratio refers to the mass percentage of each resin (NOA 1665/NOA 170), where each maintains a 50% volume fraction in the composite mix.

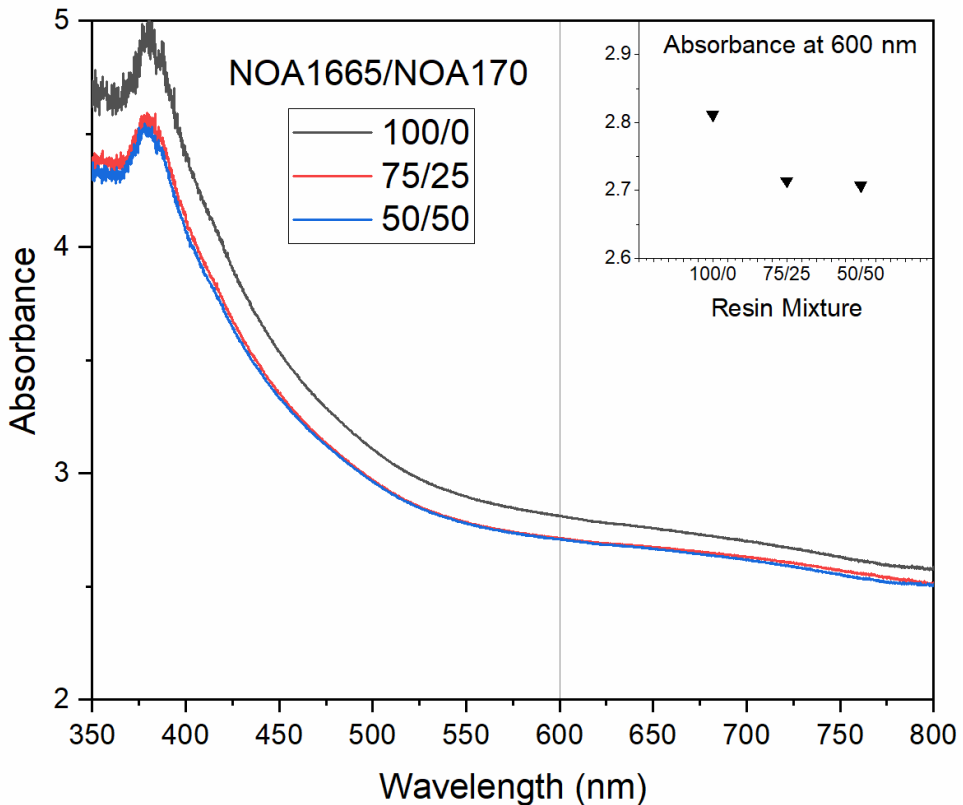


Fig. 6. UV-VIS absorption spectra of each of the composites from the mixed resin study. Resins containing any quantity of NOA 170 indicated a reduced total absorption, suggesting a more closely matched index of refraction to the BaFCl:Eu²⁺ crystals. The inset displays the absorbance at 600 nm for each composite mixture to show the linear trend.

3.3 Application of the BaFCl:Eu²⁺ Scintillator

Vital to the success of the project, it is necessary that each pixel of the screen be filled completely and that the screen be as isotropic as possible. Two methods were tested to determine which could more closely meet this requirement. The first method, utilizing the composite, relied on the kinetics of the material (i.e. viscosity) and the amount of sheer force applied to fill the holes of the screen. The alternate method utilizes the polycrystalline powder to fill the holes, and NOA 1665 was applied over to fill the voids via capillary action. Shown in Fig. 7, the results of the two trials clearly show a substantial difference in the homogeneity of the filled screen. In the top of the figure, the composite route shows decent uniformity within a selected region of the screen. In the bottom of the figure, applying the scintillator as a powder initially appeared to be highly effective, however, after applying the resin it became apparent that uniformity was an issue. Fig. 8 shows a line profile of the dashed regions from Fig. 7, and the standard deviations of the average values are provided for each region. It can be seen that the fluctuation in surface quality is nearly 4 times greater in the powder-resin application than the composite-paste application. From this trial, it is believed that the composite will provide the most uniformity across the screen, and additionally will be more translucent to visible light.

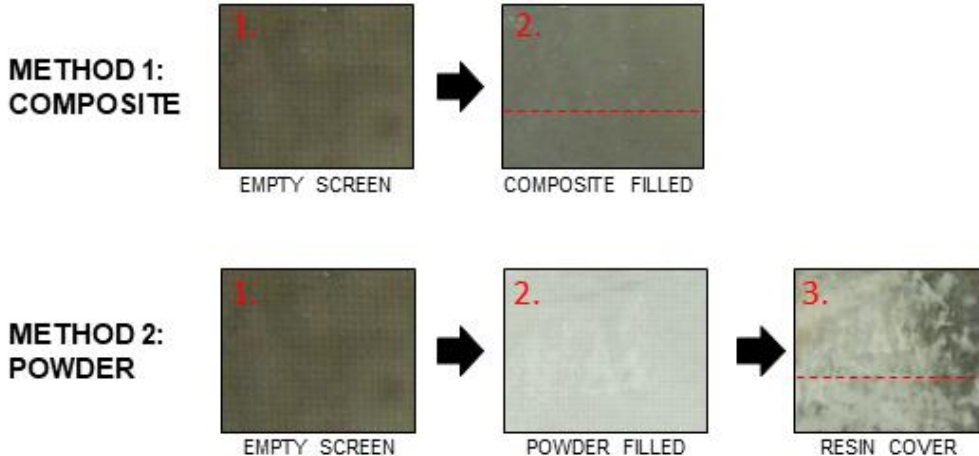


Fig. 7. Images of the pixelated glass screen before and after applying the scintillator. In method 1 (top), the BaFCl:Eu²⁺ composite was applied to the screen through sheer force. In method 2 (bottom), first BaFCl:Eu²⁺ powder was added and distributed as uniformly as possible; then NOA1665 was applied to fill any potential voids to seal the powder within the screen. As is shown, method 2 was unsuitable for completely filling each pixel uniformly. Dashed lines are included for reference of surface fluctuations analyzed in Fig. 8.

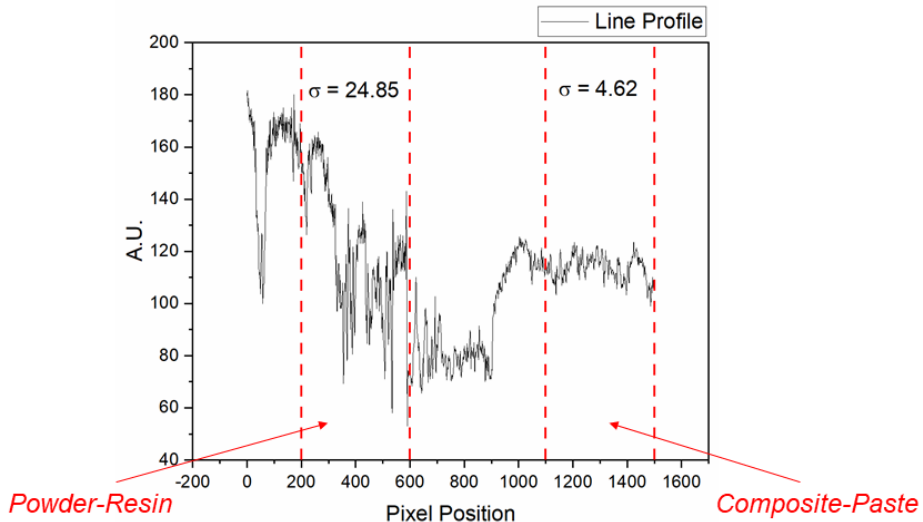


Fig. 8. Line profile of the surface height variation taken from the filled glass screen. The regions within the dashed lines correspond to the dashed lines in Fig. 6 of the filled screen. Standard deviation values of each region are provided at the top of the figure, and it can be seen the fluctuation for the powder-resin method is approximately 4x greater.

4. Conclusions

It has been shown that a large-scale flux-growth synthesis is capable of producing increased quantities of high quality BaFCl:Eu²⁺ powder. The resulting scintillator displays very bright photoluminescence and has a high quantum yield near resonance excitation. Composites containing the BaFCl:Eu²⁺ were fabricated with improved uniformity by increasing the amount of IPA included prior to mixing, but allowing ample time for it to evaporate after mixing. The translucency of the composites were also improved by incorporating NOA 170 optical adhesive into the mixture, thereby reducing the difference in index of refraction of the combined resins and the scintillator. When applying the scintillator to the pixelated screen, the composite method was shown to provide near isotropic packing of the pixelated structures.

Funding

Funding for this project was provided by Los Alamos National Laboratory.

Acknowledgments

Special thanks to Dr. Brenden Wiggins for mentorship and introduction into the scintillator field.

References

1. Chen, W., et al. (2005). "X-Ray Storage Luminescence of BaFCl:Eu²⁺ Single Crystals." *The Journal of Physical Chemistry B* 109(23): 11505-11511.
2. Chen, W., et al. (1998). "New color centers and photostimulated luminescence of BaFCl:Eu²⁺." *Journal of Physics and Chemistry of Solids* 59(1): 49-53.
3. Cusano, D. A., et al. (1983). Index-matched phosphor scintillator structures. United States.
4. Eachus, R. S., et al. (1995). "Oxygen defects in BaFBr and BaFCl." *Physical Review B* 52(6): 3941-3950.
5. Es-Sakhi, B., et al. (2002). "Photoluminescence of Eu²⁺ in BaF₂-rich fluorohalides and photostimulation after X-ray irradiation." *Materials Science and Engineering: B* 96(3): 233-239.
6. Fox, A. M. (2001). *Optical Properties of Solids*, Oxford University Press.
7. Ignatovych, M., et al. (1999). "Spectral and Dosimetric Characteristics of Eu-Doped X-Ray Phosphors." *Radiation Protection Dosimetry* 84(1-4): 185-188.
8. J Bastow, T., et al. (1999). "Oxygen impurities in X-ray storage phosphors BaFBr and BaFCl investigated by ¹⁷O NMR." *Journal of Physics: Condensed Matter* 6(41): 8633.
9. Knoll, G. F. (1999). *Radiation Detection and Measurement*. United States of America, John Wiley & Sons, Inc.
10. Körner, M., et al. (2007). "Advances in Digital Radiography: Physical Principles and System Overview." *RadioGraphics* 27(3): 675-686.
11. Kubel, F., et al. (1996). "Synthesis and Structure of Ba₁₂F₁₉Cl₅." *Zeitschrift für anorganische und allgemeine Chemie* 622(2): 343-347.
12. Leblans, P., et al. (2011). "Storage Phosphors for Medical Imaging." *Materials* (Basel, Switzerland) 4(6): 1034-1086.
13. Meng, X. and J. Zhou (2010). Photostimulated luminescence of BaFCl:Eu²⁺ in oxide glass ceramics.
14. Moy, J.-P. (2000). "Recent developments in X-ray imaging detectors." *Nuclear Instruments and Methods in Physics Research Section A: Accelerators, Spectrometers, Detectors and Associated Equipment* 442(1): 26-37.
15. Sauvage, M. (1974). "Refinement of the structures of SrFCl and BaFCl." *Acta Crystallographica Section B* 30(11): 2786-2787.
16. Secu, C. E., et al. (2007). "High temperature thermoluminescence of BaFCl:Eu²⁺ X-ray storage phosphor." *physica status solidi c* 4(3): 1016-1019.
17. Secu, M., et al. (2007). "Time-resolved luminescence spectroscopy of Eu²⁺ in BaFCl:Eu²⁺ X-ray storage phosphor." *Journal of Optoelectronics and Advanced Materials* 9(6): 1800-1802.
18. Secu, M., et al. (2000). "Preparation and optical properties of BaFCl:Eu²⁺ X-ray storage phosphor." *Optical Materials* 15(2): 115-122.
19. Shefer, E., et al. (2013). "State of the Art of CT Detectors and Sources: A Literature Review." *Current Radiology Reports* 1(1): 76-91.
20. Stevels, A. L. N. and F. Pingault (1975). "BaFCl:Eu²⁺, a new phosphor for X-ray-intensifying screens." *Philips Research Reports* 30(5): 277-290.
21. Yanagida, T. (2018). "Inorganic scintillating materials and scintillation detectors." *Proceedings of the Japan Academy. Series B, Physical and biological sciences* 94(2): 75-97.